We are IntechOpen, the world's leading publisher of Open Access books Built by scientists, for scientists

6,900
Open access books available

185,000
International authors and editors

200M
Downloads

Our authors are among the

154
Countries delivered to

TOP 1%
most cited scientists

12.2%
Contributors from top 500 universities



WEB OF SCIENCE™

Selection of our books indexed in the Book Citation Index in Web of Science™ Core Collection (BKCI)

Interested in publishing with us?
Contact book.department@intechopen.com

Numbers displayed above are based on latest data collected.
For more information visit www.intechopen.com



Chapter 2

Crystallization of the Long Biological Macro-Molecules

Uziel Sandler

Additional information is available at the end of the chapter

1. Introduction

Phase transition in molecular crystals and molecular liquids is a complicated phenomenon. The energy of intra-molecular interaction is higher than the characteristic temperatures of the transitions, so the structural transformations are determined by a competition between the inter-molecular interactions that try to put the molecules in some ordered state and tendency of the entropy to break of this order. Since the small molecules interact with small number of the neighbors, mean-field-approximation is inadequate and calculating of the free energy requires non-trivial higher approximations. Besides, the relevant parameters of the inter-molecular interactions depend on details of the molecular structure and correct estimation of them requires a complex quantum-mechanical calculation, so huge numerical calculations should be done in the real cases.

In this chapter we will consider the system that consists of the long semi-flexible macromolecules[1] or molecular aggregates (LM). We will assume also that the energy of the relevant intra-units interactions is of the same order as a characteristic temperature of the phase transformations. In such a case above mentioned complications could be avoided by using the concepts of "quasi-monomers" or "blobs" (see [13, 16] and references therein). Because of the macroscopic nature of these units, an effective inter-unit interaction are defined by their geometrical properties, while most details of the internal structure and internal interactions of the units become irrelevant. Moreover, since for the relevant densities each macro-unit interacts with large number of the neighbors, so the mean-field-approximation could be quite adequate for calculation of the most the thermodynamic characteristics and these calculations can be done analytically.

[1] A molecule will be called "long" if it length L is much more than it thickness a and "semi-flexible" if it persistent length l_p is much more than it thickness and much less than the molecule's length: $L \gg l_p \gg a$.

INTECH
open science | open minds

© 2015 The Author(s). Licensee InTech. This chapter is distributed under the terms of the Creative Commons Attribution License (http://creativecommons.org/licenses/by/3.0), which permits unrestricted use, distribution, and reproduction in any medium, provided the original work is properly cited.

2. Experimental study of phase transitions in the biological materials

2.1. The collagenous materials

A novel material was developed by exerting high pressure and temperature on natural leather material[2] in an oxygen poor environment. This material, which was called pleather, is thermoplastic [2]. The leather itself may be inexpensive scrap which is commutated into fine particles ($\sim$2 mm). By using common plastic forming techniques it is possible to mould this material into various shapes. Pleather, having a warmer feel than polymers, could replace polymers in furniture parts and prestigious packaging, where the price of genuine leather makes it use prohibitive.

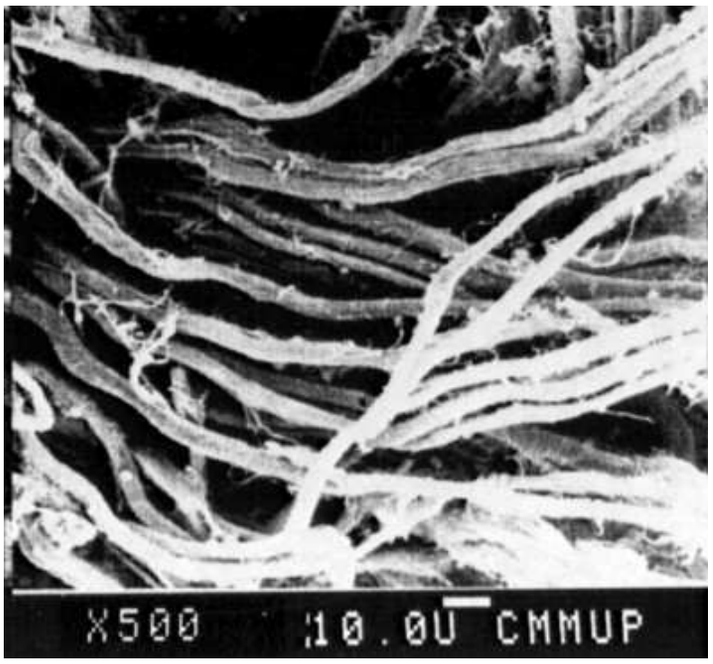


Figure 1. SEM micrograph of internal structure of *leather*. Adapted with permission from Ref. [14]. © [1995] American Physical Society.

The structure and properties of leather and their building unit, the collagen molecule, at atmospheric pressure and moderate temperatures have been extensively studied (see e.g. [8] and the bibliography there). The collagen molecule in helix form, has a length of $3000A$ and a diameter of $15A$. The three folded spirals are bonded by relatively weak, mainly hydrogen, bonds. The spiral consists of about 300 segments and each one contains approximately 3 amino-acid residues with $20-30$ Carbon and Nitrogen atoms [8]. It was shown that at temperatures $310^o - 330^oK$ the collagen molecules are reversibly denatured ("melted" [9]). The structure of collagenous material that emerges after compression at pressures between $5-30MPa$ and at temperatures $310^o - 390^oK$ have been investigated. Scanning Electron Micrographs (SEM) taken after treatment [2], at room temperature, show how the fibrous open leather structure transforms into a composite matrix, where left over fibers are

[2] The term leather pertains to hides from cow and sheep that are chemically treated to make it stronger and to give more resistance to heat.

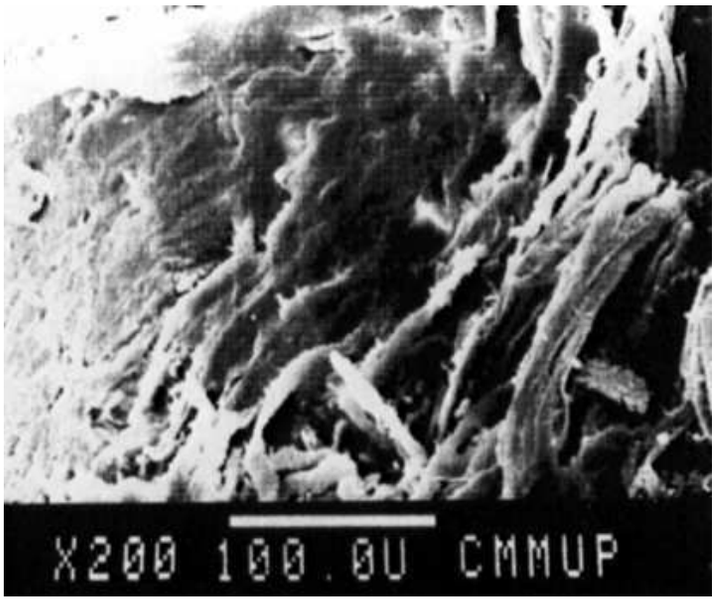


Figure 2. SEM micrograph of *compressed leather* at room temperature. Pressure: $750atm$ Adapted with permission from Ref. [14]. ℗ [1995] American Physical Society.

embedded in a continuous material (see Fig.1, Fig.2 and article [12]). By chromatography and electrophoresis methods it was shown that harsher processing conditions (higher temperature and pressure) produce an extensive degradation of the collagen superstructure, without degradation of the amino acid chains of the collagen molecule.

The biochemical [12] and mechanical properties of the material, compression strength, Young's modulus and bulk density have been studied at various processing parameters [4]. The effect of pressure on the sol-gel transition in an aqueous solution of collagen (gelatin) has been investigated in [11]. It was found, that high pressure shifts the temperature interval of collagen denaturation to higher temperatures.If the temperature is low ($T \ll T_{d1}$, where $T_{d1} \approx 310^o K$) the helix form is stable. At higher temperature, hydrogen and other weak bonds, which stabilize the helix form, become unstable and the helix breaks down to random coils [8]. This transition, however, is not sharp, but spreads over a temperature interval of $30^o - 40^o K$. This indicates that a cooperative process takes place and not a real phase transition [9]. For higher temperature ($T \geq T_{d2}$, $T_{d2} \approx 350^o K$) collagen molecules are "melted" completely. This process of the breakdown of the ordered helix structure, held together by non-covalent bonds, to a randomly coiled phase is called denaturation. The organized fibers are stable for $T \ll T_{d1}$ and break down for $T \geq T_{d2}$.

2.2. Crystallization of bacterial DNA

Bacterial DNA is an important example of a closed circular macromolecule. Although the tightly packed crystalline state is generally considered as incompatible with life, simple living systems use crystallization for different purposes. In viruses and bacteriophages DNA crystallization is used for accommodating large amounts of DNA in a very small volume. Bacteria use crystallization for protection against varied environmental assaults, thus promoting their endurance and virulence [17, 18, 29]. DNA condensation was

extensively studied during the last decade. This phenomenon has been found to be complicated, strictly depending on the DNA's topology and the cytoplasm's composition [17, 19] and involving the influence of different forces [20, 21]. DNA crystallization includes many processes and could lead to different condensed states: liquid crystals, DNA-protein co-crystals, DNA toroid [17, 18, 22].

DNA crystallization was studied in wild-type Escherichia coli AB1157 (recA1,lexA1) as well as various recA mutants, which were grown to midlogarithmic phasein LB medium without NaCl. Cultures then were exposed to DNA-damaging agents like UV irradiation (20 Jym2, 254 nm) or 100 mg of nalidixic acid. The cells were incubated at 37řC for different times from 15 to 120 min, afterwards the E.coli cells were fixed by ultrafast freezing in liquid ethane. For each time point 3 independent experiments were conducted and about 10^3 cell slices were screened. After a wash with the blocking solution, the grids were incubated with gold-conjugated goat antirabbit IgG for 1 h, dried, and stained with uranyl acetate. Images of the intracellular crystals were digitized with an Imacon Flextight scanner [18].

In the SEM micrographs bacterial chromatin of the active cells is demarcated as amorphous spaces, which are irregularly spread over the cytoplasm. After exposing to DNA-damaging agents, the cells show the SOS response, where the DNA breaks by stalling its activity. Continuous addition of nalidixic acid leads to an expansion of the assembly, whose average length increases up to 4 times after 60 min. Further incubation does not affect an expansion but results in a higher lateral order. The crystalline morphology of bacteria that have sustained prolonged exposure to DNA-damaging agents is clear seen in Fig.3.

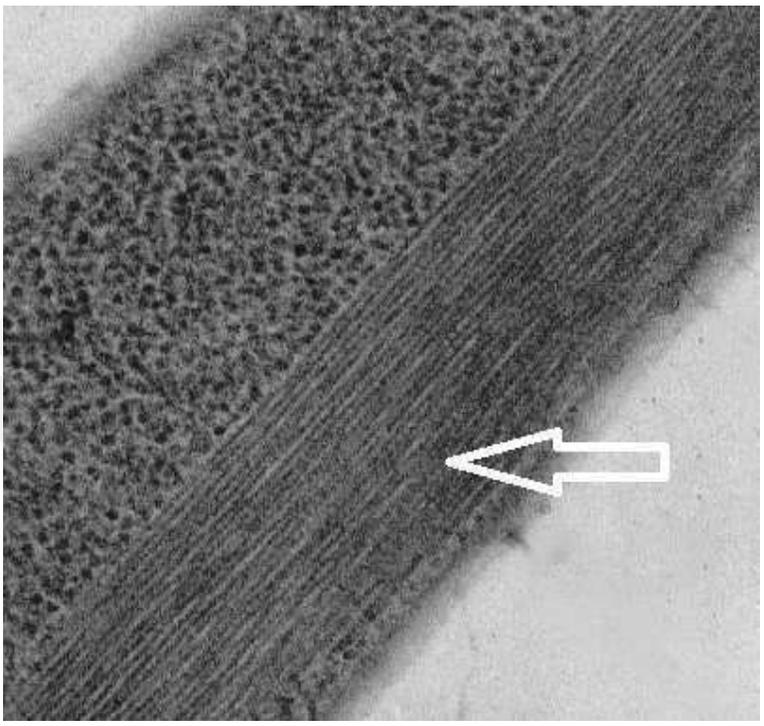


Figure 3. SEM micrograph of E. coli has been exposed to DNA-damaging agents. The array shows crystallized DNA. Adapted with permission of the author from Ref.[18].

3. Qualitative consideration of the theoretical approach

It is well known [6] that properties of phase transition in the polymer and liquid crystal systems are determined by general characteristics of the molecule's geometry and analytical behavior of the intermolecular forces, while particular details of these features are less relevant. So, we can assume that near the phase transition the major factors that determine the process of the LM crystallization are the topology of the LM molecule and the behavior of the effective LM's segment-segment interactions.

The liquid-crystal ordering of a LM is determined by the angular-dependence of interactions between LM segments. At low density, the LM pieces interact only at a small number of points, but when the solvent approaches the crossover point the number of collision points increases. When typical length between the collision points become approximately the same as the persistent length, the rigidity of a long molecule becomes important and there is a tendency to align quasi-straight pieces with quasi-parallel structure. This means that in the high density state of LM the phase transition from disordered to liquid-crystal-like ordered phase [5], should take place.

Let us estimate critical volume fraction of the molecules near crystallization point. The average number of binary collisions between LM quasi-straight pieces can be estimated as:

$$k_L \sim N \left(\frac{L}{l_p} \right)^2 v, \tag{1}$$

where N is number of the molecules in the volume V and v is an interaction volume. So, we have

$$k_L \sim L \frac{cv}{a^2 l_p^2}, \tag{2}$$

where - c is the volume fraction of LM segments. On the other hand, the average distance between collision points is on the order of:

$$\bar{l}_k \sim \frac{L}{k_L} \sim \frac{a^2 l_p^2}{cv}. \tag{3}$$

Critical volume fraction - c_*, where structural phase transition could take place, can be estimated from $\bar{l}_k \sim l_p$

$$c_* \sim \frac{a^2 l_p}{v}$$

Since part of the LM shorter than l_p can be considered as an almost rigid rod, for v we can use an excluded volume approximation $v \sim l_p^2 a$, which leads to

$$c_* \sim \frac{a}{l_p}. \tag{4}$$

This "naive" estimation is consistent with more rigorous calculations for the liquid-crystal ordering of long semi-flexible molecules under pressure (see Sec.4.1).

4. Crystallization of the collagenous materials

4.1. A phase transition under pressure at low temperatures

Although the main assumptions of our theory are general enough to apply to a whole class of compressed materials made from various natural or artificial fibers, we will discuss here a concrete case of collagen made material - natural leather, which is made up of fibers of the collagen molecules (see Section 2.1). At low temperature the fibers are stable and can be considered as basic units. If the volume fraction of fibers - c, is relatively small which occurs at low pressure, the fibers intermingle in a disordered way and interact only at a relatively small number of points (see Fig.1). When the pressure is increased the number of fibers per volume fraction increases and the interaction between the fibers becomes important.

If we designate a typical coefficient of elasticity per unit of length of fiber as γ, the persistence length (quasi-straight pieces) l_p, will be of order γ/T where T is the temperature. The condition, that l_p is much longer than the diameter a of the fibers, can be expressed as $aT/\gamma \ll 1$. It can also be seen from the SEM micrographs Fig.1, that the typical length of fiber L is much longer than l_p. So $LT/\gamma \gg 1$. The energy of a fiber consists of its elastic energy and the energy of interaction with other fibers. It follows from experimental data [12],[2] that an ordered phase appears for quite a large value the of fiber's volume fraction. In this case repulsive short-range forces between fibers are dominant. It is obvious also that the interaction between two quasi-straight pieces depends on the angle between them.

In the mean field approximation (MFA) the angular dependent part of the energy of interaction between one fiber and the others can then be represented in the form:

$$\Delta U_i = \int_0^L dl\ U[\boldsymbol{s}_i(l)]$$

where

$$U(\boldsymbol{s}) = \frac{Tc}{a} \int_{\boldsymbol{n}^2=1} d\boldsymbol{n}\ S(\boldsymbol{n}) u\left(\boldsymbol{s};\boldsymbol{n}\right)) \tag{5}$$

Here $\boldsymbol{s}_i(l)$ is the unit tangent vector of the fiber (i) at a distance l from the beginning of the fiber, $S(\boldsymbol{n})$ is the average fraction of the quasi-straight pieces of the fibers that are directed in the direction $\boldsymbol{n}$ and $Tcu(\boldsymbol{s},\boldsymbol{n})/a$ is the angular dependent interaction between two pieces of fibers.

If we assume the simplest form for the elastic energy of the fibers (isotropic approximation), than in the lowest order on a/l_p part of the energy, which depends on the local orientation of the fiber pieces will be:

$$\Delta\mathcal{E}_{MFA} = \frac{1}{2}\sum_i^N \int_0^L dl \left\{ \gamma \left(\frac{\partial \boldsymbol{s}_i}{\partial l} \right)^2 + U[\boldsymbol{s}_i(l)] \right\} \tag{6}$$

where N is the total number of fibers. The free energy of the system can be expressed as path integral over all the possible shapes of the fibers:

$$\mathcal{F} = \mathcal{F}_0 - T \ln \left[\int \prod_i \mathcal{D}\{\boldsymbol{s}_i(l)\} \exp\left(-\frac{\Delta \mathcal{E}_{MFA}}{T} \right) \right] \tag{7}$$

where $\mathcal{F}_0$ is the part of free energy which does not depend on the elasticity and shapes of the fibers.

In the usual way[3] the path integral (7) may be written in the form:

$$\mathcal{F} = \mathcal{F}_0 - N \ln \left(\sum_n \exp -E_n L \right) \tag{8}$$

where E_n is the eigne-value of the Schrodinger-like equation associated with this path integral

$$\frac{\partial \psi}{\partial l} = \frac{T}{2\gamma} \nabla^2_{\boldsymbol{s}} \psi - \frac{U(\boldsymbol{s})}{2T} \psi \tag{9}$$

here $\boldsymbol{s}$ is a unit vector and $\nabla^2_{\boldsymbol{s}} = \partial^2/\partial\theta^2 + \tan^{-1}\theta \partial\theta + \sin^{-2}\theta \partial^2/\partial\varphi^2$ is the angular part of the Laplacian operator.

In the ordered phase the “depth of the potential well - $(U_{max} - U_{min})/2T$" is large compared to the “kinetic energy -$T/2\gamma$", because, the phase transition to the ordered phase occurs for $c \sim 1$ [2] and

$$max\left(\frac{\gamma}{T^2} U \right) \sim \frac{c\gamma}{aT} \sim c \frac{l_p}{a} \gg 1.$$

while $min(U) \approx 0$. On the other hand, in a disordered phase $S(\boldsymbol{n}) \equiv 1/4\pi$ and $U(\boldsymbol{s}) = const$. In both cases the energy spectrum will be discrete and the gap between the ground state and the 1st exited state will be about

$$E_1 - E_0 \sim \frac{T}{\gamma}.$$

As $LT/\gamma \sim L/l_p \gg 1$, the ground state is dominant, and we obtain for the free energy per unit volume

$$F = F_0 + \frac{Tc}{a^2} E_0 \tag{10}$$

and for $S(\boldsymbol{n})$

$$S(\boldsymbol{n}) = |\psi_0(\boldsymbol{n})|^2 = \Psi^2(\boldsymbol{n}) \tag{11}$$

[3] See more precise consideration in Sec.5

E_0 can be obtained by using the variation principle from which we find that

$$F = F_0 + \frac{Tc}{2a^2}\int d\boldsymbol{s}\left[\frac{T}{\gamma}\left(\frac{\partial\Psi}{\partial\boldsymbol{s}}\right)^2 + \frac{c}{a}\int d\boldsymbol{n}\Psi^2(\boldsymbol{s})u(\boldsymbol{s};\boldsymbol{n})\Psi^2(\boldsymbol{n})\right] \tag{12}$$

This is a well known Ψ^4 field Hamiltonian. The function $\Psi(\boldsymbol{s})$ must be found by minimizing F under the restriction

$$\int d\boldsymbol{s}\Psi^2 = 1 \tag{13}$$

It can be done in many ways. Here we will use the simple approximation, which Onsager used in his treatment of liquid crystals [5]. In this approximation it is assumed that $\Psi(\boldsymbol{s})$ is a narrow peaked function in an ordered phase

$$\Psi(\boldsymbol{s}) = \phi\left(\lambda(\boldsymbol{s}\cdot\boldsymbol{s}_0)\right) \qquad (\lambda \gg 1) \tag{14}$$

where $\boldsymbol{s}_0$ is the direction of an average orientation of the quasi-straight pieces, while in a disordered phase $\Psi(\boldsymbol{s}) \equiv \sqrt{1/4\pi}$ (this means that in a disordered phase $\lambda = 0$) [4]. The parameter λ should be found by minimizing F.

The difference between the free energy in the ordered and disordered phases is

$$\Delta F \simeq \frac{Tc^2}{2a^3}\left\{g\left(\frac{Ta}{\gamma c}\right) - 1\right\} \tag{15}$$

where the specific form of the function $g(x)$ depends on the behavior of $u(\boldsymbol{s},\boldsymbol{n})$ near $\boldsymbol{s} \approx \boldsymbol{n}$. If it is assumed that near $\boldsymbol{s} \approx \boldsymbol{n}$ the behavior of $u(\boldsymbol{s},\boldsymbol{n})$ is of the form

$$f \propto \eta[\boldsymbol{s}\times\boldsymbol{n}]^{2\nu} \tag{16}$$

(η is a constant $O(1)$), then in the Onsager approximation one finds[5]

$$g(x) \approx (\mu x)^{\frac{\nu}{1+\nu}} \tag{17}$$

with

$$\mu \approx (4\kappa\nu\eta)^{\frac{1}{\nu}} \tag{18}$$

[4] Onsager used the function ϕ in the form $\phi(x) = A\cosh(\lambda x)$, but the final results are weakly sensitive to the concrete form of $\phi(x)$.

[5] The parameter λ here is

$$\lambda = \begin{cases} \left(4\nu ac\frac{T_*}{T}\right)^{1/1+\nu} \gg 1 & \text{if } T < T_*c \\ 0 & \text{if } T > T_*c \end{cases}$$

which justifies the use of the approximation (14)

The numerical coefficient κ is $O(1)$ and depend on the explicit form of the test function (14).

It is obvious from (15), that for fixed T and a specific value of the fiber fraction

$$c_* = \frac{T}{T_*} \tag{19}$$

where

$$T_* = \frac{\gamma}{\mu a}$$

the material undergoes a first order phase transition from the disordered to the ordered phase. The ordered phase is stable for $T < T_*$ and it is called *compressed leather* (see Fig.2).

The order parameter $\mathcal{Q}$, that describes the ordering in the orientation of the fibers, can be defined as

$$\mathcal{Q} \approx \frac{1}{2}\left(3\int d\boldsymbol{n} S(\boldsymbol{n})(\boldsymbol{n}\cdot\boldsymbol{s}_0)^2 - 1\right) \tag{20}$$

In the ordered phase using (11) with $\Psi(\boldsymbol{n})$ from (14) one obtains

$$\mathcal{Q} \approx 1 - \frac{3}{\lambda} \approx 1 - 3(4\nu a)^{-1/1+\nu}\left(\frac{T}{T_* c}\right)^{\frac{1}{1+\nu}} \tag{21}$$

(in the disordered phase $\mathcal{Q} = 0$). The difference between thermodynamic parameters of the ordered and disordered phase can be obtained as follows

$$q \sim \frac{T_*}{a^3}\frac{\nu}{1+\nu}\left(\frac{T}{T_*}\right)^3 \tag{22}$$

$$\Delta C \sim \frac{1}{a^3}\frac{\nu(1+2\nu)}{(1+\nu)^2}\left(\frac{T}{T_*}\right)^{\frac{\nu}{1+\nu}} c^{\frac{2+\nu}{1+\nu}} \tag{23}$$

$$\Delta K_B \sim \frac{Tc^2}{a^3}\left(1 - \frac{2+\nu}{2(1+\nu)^2}\left(\frac{T}{T_* c}\right)^{\frac{\nu}{1+\nu}}\right) \tag{24}$$

where q is the latent heat, C is the specific heat, K_B is the bulk modules, and Δ indicates the difference between ordered and disordered phase. In general, the ordered phase consists of domains with different fiber orientation (see Fig.2) but the energy of the domain boundaries gives a small contribution to ΔF.

It should be noted, that for large volume fraction of the collagen fibers the form of their cross sections changes, and therefore so do the effective diameter and elasticity. Furthermore, the elasticity of the fiber bundles and coefficient ρ in the expression (12) depend on temperature,

so that we must consider $T_* = T_*(T, c)$. If T is less than T_{d1} (T_{d1} is the lowest temperature of collagen denaturation: $T_{d1} \sim 350^0 K$) the inner structure of the fibers almost doesn't change and the dependence $T_* = T_*(T, c)$ is quite weak. In general such dependence does not change the expressions for the free energy and order parameter, but additional terms appear in the other thermodynamic quantities. However, as most of the expressions contains T_* in a low power they are relatively insensitive to its variations. It is not anticipated that a change from the isotropic approximation for the elastic energy to a more realistic approximation would produce changes of any significance.

4.2. A phase transition under increasing temperature at high pressure

If we increase the temperature of *compressed leather* with fixed c, to a temperature higher than $T_0 = cT_*$ a first order phase transition from the ordered to the disordered phase takes place. If $T_0 \ll T_{d1}$ this phase will be *leather*. A more complex situation occurs for $T_0 > T_{d1}$. If the temperature is higher than T_{d1} the helix form of the collagen molecule becomes unstable, the molecules melt and the fibers are destroyed. The approach of the previous Section fails, because the variation in the internal free energy of the fibers plays a major role [10]. The structure of the material for $T \geq T_{d1}$ is determined by the competition between the melting and ordering of the collagen molecules. We will describe the behavior of the material by using the following model.

In a first approximation the leading term of the free energy can be represented as

$$F = F_0 + cf_{mol} + Tce_{orien} + F_{int} \tag{25}$$

where f_{mol} is the free energy of a single collagen molecule, e_{orien} is the orientation dependent part of the entropy and F_{int} is the energy of intermolecular interaction. In order to calculate f_{mol} we use an approximation which is close to the well-known Zimm-Bragg model. The latter is in good agreement with the real behavior of the collagen molecules (see, for example [9]).

Consider a collagen molecule that contains sN segments in helix form and pN boundaries between "helix" and "coil" parts of the molecule (in the literature s is called spirality), where N is the number of segments in the molecule. N is large. Let us call the free energy of a segment in helix form - ε_h, in coil form - ε_c and the energy of segments on the boundary between helix and coil parts as ε_s ($\varepsilon_h - \varepsilon_c = \Delta U - T\Delta S \equiv \Delta S\,(T_m - T)$, where ΔU and ΔS are the differences between the internal energy and entropy of a spiral and a melted segment). As the collagen molecule can be considered as a one-dimensional system, we can calculate the free energy f_{mol} in an analogous way as for the 1D-Ising model. The result is [9]:

$$f_{mol} = -\left(\varepsilon_c - \varepsilon_h\right) s + \varepsilon_s p - T\left\{s \ln s + (1-s)\ln(1-s) - \right. \tag{26}$$

$$\left. -2p \ln p - (s-p)\ln(s-p) - (1-s-p)\ln(1-s-p)\right\} \tag{27}$$

The last two terms in (25) can be obtained in the MFA approximation (see Sec.4.1)

$$e_{orien} = s \int_{\boldsymbol{n}^2=1} d\boldsymbol{n}\; g(\boldsymbol{n}) \ln\left(4\pi g(\boldsymbol{n})\right); \tag{28}$$

$$F_{int} = \frac{c^2}{2}\left\{ s^2 \int_{\boldsymbol{n}^2=1} d\boldsymbol{k} d\boldsymbol{n} g(\boldsymbol{k}) g(\boldsymbol{n}) U(\boldsymbol{k};\boldsymbol{n}) + 2T\chi_{sh} s\,(1-s) + T\chi_{ss}\,(1-s)^2 \right\} \tag{29}$$

where $g(\boldsymbol{n})$ is the average fraction of the segments in helix form that are directed in the direction $\boldsymbol{n}$. The first term in (29) corresponds to the interaction between helix-helix segments, while the others describe the interaction between helix-coil and coil-coil segments resp.

The energy of interaction between spiral segments we write in the form

$$U(\boldsymbol{k};\boldsymbol{n}) \simeq T\chi_{hh} u(\boldsymbol{k};\boldsymbol{n}), \tag{30}$$

We assume as above, that near $\boldsymbol{k} \approx \boldsymbol{n}$

$$u \propto |\boldsymbol{k} \times \boldsymbol{n}|^{2\omega}, \tag{31}$$

which corresponds to a repulsive interaction in an excluded-volume approximation[6]. In this approximation, $\omega = 0$ corresponds to the bundles made from hard spheres, $\omega = 0.5$ to the bundles made from hard bars, $\omega = 1$ corresponds to MaierŰSaupe approximation and larger ω may be used for arch-like "hemstitch" units. We will also assume that in a first approximation the coefficients $\chi_{hh} \approx \chi_{hs} \approx \chi_{ss} \approx n_s\chi$ are of the same order. n_s is the number of atoms in the segments.

Using Onsager approximation for $g(\boldsymbol{k})$ [5] and integrating (29) over $\boldsymbol{n}$ and $\boldsymbol{k}$, we obtain for $\lambda \gg 1$:

$$Tce_{orien} + F_{int} \simeq Tc\left\{ s\,(\ln\lambda - 1) + s^2 \frac{cn_s\chi}{2} \zeta\,(\omega)\,\lambda^{-\omega} - s^2 \frac{cn_s\chi}{2} \right\} + \frac{Tc^2 n_s\chi}{2} \tag{32}$$

where coefficient $\zeta\,(\omega)$ is (see Appendix 1)

$$\zeta\,(\omega) = 2^{2\omega+1}\pi^{-1/2}\Gamma\left(\frac{3}{2}+\omega\right).$$

[6] In fact, $U(\boldsymbol{k};\boldsymbol{n})$ must includes the term that corresponds to an attractive interaction. This term has the form:

$$\delta U \sim -\frac{p}{s}\mu u_{attr}(\boldsymbol{k};\boldsymbol{n}).$$

In our theory, however, δU can be neglected for the following reasons: for $s \leq 1$ and $\varepsilon_s \gg \varepsilon_c - \varepsilon_h$, δU is small because $p \ll s$. On the other hand, if $s \ll 1$ and $p \sim s$ the whole term $s^2 \int_{\boldsymbol{n}^2=1} d\boldsymbol{k} d\boldsymbol{n} g(\boldsymbol{k}) g(\boldsymbol{n}) U(\boldsymbol{k};\boldsymbol{n})$ in (29) is small and can be neglected.

In the disordered phase $g(\boldsymbol{k}) \equiv 1/4\pi$ and the interaction term in this approximation does not depend on spirality:

$$F'_{int} = \frac{Tc^2}{2}\left\{\chi_{hh}s^2 + 2\chi_{sh}s\,(1-s) + \chi_{ss}\,(1-s)^2\right\} \approx \frac{Tc^2 n_s \chi}{2}. \tag{33}$$

In the ordered phase the quantities s, p and λ have to be found by minimizing (25). This gives

$$\lambda = \left(\frac{c}{c_0}\right)^{1/\omega} s^{1/\omega}, \tag{34}$$

$$\frac{(1-s-p)\,s}{(s-p)\,(1-s)} = \frac{\lambda}{\tau}\exp\frac{2}{\omega}\left(-\frac{c}{\zeta c_0}s + 1 - \frac{\omega}{2}\right), \tag{35}$$

$$\frac{p^2}{(s-p)\,(1-s-p)} = \sigma, \tag{36}$$

where

$$\tau = \exp\frac{\varepsilon_c - \varepsilon_h}{T} \equiv \exp\Delta S\frac{T_m - T}{T},$$

$$\sigma = \exp -\frac{\varepsilon_s}{T}, \tag{37}$$

$$c_0 = \frac{2}{\chi n_s \omega \zeta}. \tag{38}$$

(for collagen $\varepsilon_s \gg T_m, \omega \approx 0.5$, $n_s \sim 2\cdot 10^1$ and $\Delta S \sim 10$). If $cs \ll c_0$, λ is small and the above used approach fails. For such c and s however, the angle-dependent interaction between molecules becomes irrelevant, and the system will be in the disordered phase. In this phase $\lambda = 0$ and the free energy F' can be calculated in an explicit form. The result is [9]

$$F' \approx F_0 - cT\ln\frac{\tau + 1 + \sqrt{(\tau-1)^2 + 4\sigma\tau}}{2} + \frac{Tc^2 n_s \chi}{2}. \tag{39}$$

The order parameter in the ordered phase is

$$\mathcal{Q} \approx 1 - \frac{3}{\lambda} + o\left(\frac{1}{\lambda^2}\right) \simeq 1 - 3\left(\frac{c_0}{c}\right)^{1/\omega} s^{-1/\omega}. \tag{40}$$

Note, that we have here

$$\frac{\partial \ln(1-\mathcal{Q})}{\partial \ln c} = \frac{\partial \ln(1-\mathcal{Q})}{\partial \ln s} \approx -\frac{1}{\omega}, \tag{41}$$

while for the phase transition under pressure at low temperatures it is obtained in Sec.4.1 that:

$$\frac{\partial \ln(1-\mathcal{Q})}{\partial \ln c} \approx -\frac{1}{1+\nu}, \tag{42}$$

So in (41) the dependence of $\mathcal{Q}$ on ω is much stronger for small ω, than the dependence of $\mathcal{Q}$ on small ν in (21). These derivations depend only on ω or ν and thus measurement of $\mathcal{Q}$ gives important information on the type of inter-fiber interaction.

The solution of the system (34)-(36) that corresponds to large λ, is

$$1-s \approx \frac{1}{\tau}\left(\left(\frac{c}{c_0}\right)\exp\left(-\frac{2c}{\zeta c_0}+2-\omega\right)\right)^{\frac{1}{\omega}} \ll 1$$

$$\mathcal{Q} \approx 1-3\left(\frac{c}{c_0}\right)^{-\frac{1}{\omega}}. \tag{43}$$

The phase transition temperature - T_c is found from the condition $F_{order}(T_c) = F'_{disorder}(T_c)$. So we obtain:

$$\Delta S \frac{T_c - T_m}{T}_c \simeq \xi\left(\omega, \frac{c}{c\,t}\right) - \ln\left(1+\frac{\sigma e^{-2\xi}}{1-e^{-\xi}}\right), \tag{44}$$

$$\xi \approx \frac{\rho(\omega)(c/c_t - 1) - \ln(c/c_t)}{\omega},$$

$$\rho = \ln\rho + \ln\zeta(\omega)\, e^{1-\omega}, \tag{45}$$

$$c_t = \zeta\rho c_0. \tag{46}$$

The ordered phase can be stable only if $c > c_t = \zeta\rho c_0$. Thus $\lambda > (\zeta\rho)^{1/\omega}$ and the above used approximation (32) is valid, because $\zeta\rho > 1$.

The derivative of the transition temperature to the pressure

$$\frac{\partial T_c}{\partial P} \propto \frac{\partial T_c}{\partial c} \sim \frac{T_c^3}{q\omega T_m}\left(1+\sigma\frac{\left(2-e^{-\xi}\right)e^{-2\xi}}{\left(1-e^{-\xi}\right)^2}\right)\left(\frac{c_t}{c}\right)\left(\rho\frac{c}{c_t}-1\right) > 0 \tag{47}$$

is positive. The latent heat and the jump in compressibility for this case are

$$q \sim c_t T_c \Delta S \tag{48}$$

$$\Delta\kappa \propto \frac{c_t T_c}{\omega}\left(1 - 2\rho\frac{c}{c_t}\right) < 0. \tag{49}$$

For the jumps in the orientation order parameter and in the spirality we have

$$\Delta\mathcal{Q} \simeq 1 - 3\left(\frac{c_t}{\zeta\rho c}\right)^{\frac{1}{\omega}},$$

$$\Delta s \simeq 1 - \exp\frac{1}{\omega}\left(1 - \rho\frac{c}{c_t}\right), \tag{50}$$

so the phase transition is of first order. Note, that in our approximation these jumps strongly depend on the exponent of the small-angle interaction between the molecules segments.

The restriction $c_t \leq 1$ leads to

$$n_s \geq n_{s0}(\omega) = \frac{2\rho}{\chi\omega} \tag{51}$$

and for $n_s < n_{s0}(\omega)$ the phase transition does not exist.

The numerical solution of the system (34)-(36) is shown in Fig.4. On the left hand side ($c < c_t$) cooperative "melting" takes place, while on the right hand side ($c > c_t$) a first order phase transition can clearly be seen. The inter-molecular interaction transforms the cooperative "melting" to the phase transition of the first order.

5. Crystallization of a Closed Long Macromolecule

In the previous Section we have discussed crystallization of the long open macromolecules, even though closed long macromolecules (CLM) are also widespread components of living systems. Major efforts in these and many other works were put forth to understand the peculiarities, structures and thermodynamics of condensed states of CLM. In contrast, the present paper focuses on the phase transition to a crystalline state and on the behavior of its general characteristics, like jumps of the CLM local density, the liquid crystal order parameter and transition entropy, which are biologically significant, because DNA packaging capacity and sharpness of the transition directly influence bacteria protection efficiency [17].

It is well known [6] that properties of phase transition in the polymer and crystal systems are determined by general characteristics of the molecule's geometry and analytical behavior of the intermolecular forces, while particular details of these features are less relevant. So, we can assume that near the phase transition the major factors that determine the process of the CLM crystallization are the topology of the CLM molecule and the behavior of the effective

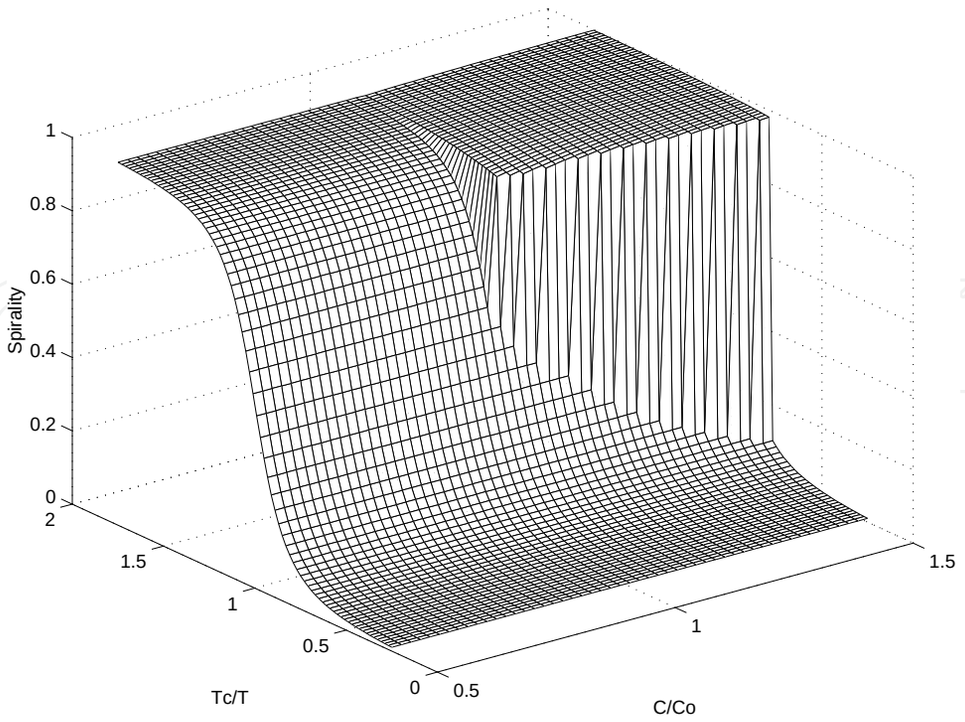


Figure 4. Spirality as a function of the normalized inverse temperature and volume fraction of the molecules. Adapted with permission from Ref. [14]. ℓ [2000] American Physical Society.

CLM's segment-segment interactions. The condensation process of a long macromolecule includes two phenomena: collapse of the molecule's chain and structural ordering of the long semi-flexible molecule's segments. Separately, each of these phenomena has been discussed in literature [6, 13, 16, 27], but, as we will see later, these processes influence each other, so their combined consideration leads to considerable change in the theoretical approach.

Consider a long closed macromolecule with a hard-core diameter a, persistent lengths l_p and total length L. (For bacterial DNA: $l_p/L \sim 10^{-4}$, $a/l_p \sim 10^{-2}$). Above the crossover point between good and poor solvent, an effective repulsion between CLM segments dominates over effective attraction and CLM remains in a low density "coil" state. Near the crossover point, segment-solvent interactions compensate contribution of binary segment-segment repulsion, so that below the crossover the effective attraction becomes dominant and the molecule undergoes transition into a compact globular form. Since segment-solvent interactions are independent of the segments' orientations, such compensation takes place only for angular-independent contributions to binary collisions.

In contrast, the liquid-crystal ordering of a CLM is determined by the angular-dependence of interactions between CLM segments. At low density, the CLM pieces interact only at a small number of points, but when the solvent approaches the crossover point the number of collision points increases. When typical length between the collision points become approximately the same as the persistent length, the rigidity of a CLM molecule becomes important and there is a tendency to align quasi-straight pieces with quasi-parallel structure. This means that in the high density state of CLM the phase transition from disordered to liquid-crystal-like ordered phase [5], should take place. However, "naive" estimation (4) is even qualitatively incorrect in the case of the condensation of a long macromolecule. In the liquid-crystal ordering that is accompanied by molecular collapse in a poor solvent,

non-binary interactions should be taken into account and the critical volume fraction is given by (see below):

$$\rho_c \sim \left(\frac{a}{l_p}\right)^{\frac{\omega}{1+2\omega}} \gg \rho_*, \tag{52}$$

where quantity ω is determined by a small-angle-limit of angular-dependent interactions between two CLM segments [15].

The Hamiltonian of a DNA molecule in bacteria is very complicated and includes many variables describing a DNA molecule, solvent components and DNA associated proteins. It can be simplified, however, by integrating the microscopic Hamiltonian over the solvent and the protein's degrees of freedom. Of course, the resulting Hamiltonian will still be sophisticated and will include nonlinear terms with derivatives and terms with nonlocal segment-segment interaction. Near the transition point, however, where the CLM density ρ is of the order of $o(a/l_p, \bar{K}l_p)$ (where $\bar{K}$ is an average local curvature of the molecule, see later), the nonlinear derivative terms can be omitted for the lowest approximation on a/l_p, $\bar{K}l_p$, while nonlocal contribution to the segment-segment interactions can be treated by using self-consisting-field approximation, which is, apparently, valid in the transition region (see below and corresponding discussion in [14]).

We will assume that the molecule's core is twisted around its centerline, so in a mechanical equilibrium state the molecule is super-coiled [23, 25] (Fig. 5). Since for bacterial DNA: $\bar{K}l_p \lesssim 10^{-1}$ [23], we will consider a case: $a/l_p \ll 1$, $l_p/L \ll 1$ and $\bar{K}l_p \ll 1$.

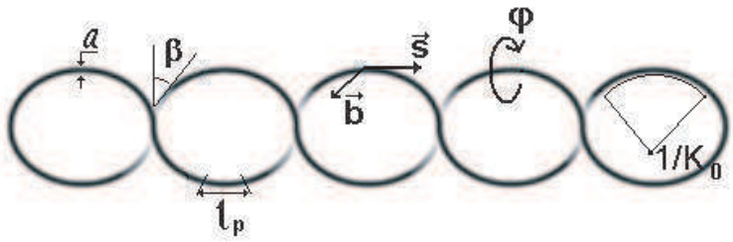


Figure 5. Super-coiled macromolecule. l_p is the effective bending persistent lengths, $\boldsymbol{s}$ is a unit tangent vector and $\boldsymbol{b}$ is a unit bi-normal vector. β is the opening angle of the super-helix, a is the hard-core diameter, φ is the twist angle and K_0 is a local curvature. Reproduced with permission from Ref.[15].

For the lowest order on a/l_p and $K_0 l_p$ energy of deformation of the super-coiled CLM can be approximated as [15]:

$$\frac{\mathcal{H}_S}{T} = \int_0^L \left\{ \frac{l_p}{2}\left(\frac{d\boldsymbol{s}}{dl} - K_0(l)[\boldsymbol{s}\times\boldsymbol{b}]\right)^2 + \frac{l_t}{2}\left(\frac{d\varphi}{dl} - \Omega_0(l)\right)^2 \right\} dl,$$

where the molecule is considered as a semi-flexible chain, with the contour parameter l and the contour length L. l_p and l_t are the effective bending and torsion persistent lengths ($l_p \sim l_t$). $\boldsymbol{s}(l)$ is a unit tangent vector at the point l and $\boldsymbol{b}(l)$ is a corresponding unit bi-normal vector. $\varphi(l)$ is the twist angle. Note that $\boldsymbol{b}, \boldsymbol{s}$ and φ are related as $d\boldsymbol{b}/d\varphi = [\boldsymbol{s}\times\boldsymbol{b}]$. The terms are proportional to K_0 and Ω_0 ensure minimum of $\mathcal{H}_S$ at an initial super-coiled state with local curvature $K_0(l)$ and local twist per unit length $\Omega_0(l)$.

The effective energy of interactions between the molecule pieces and the molecule and solvent components can be taken into account by adding an effective field U, induced by the renormalized segment-segment interactions:

$$\mathcal{H}_{PT} = \mathcal{H}_S + \frac{1}{a}\int_0^L U(\boldsymbol{x}(l), \boldsymbol{s}(l), \varphi(l))dl,$$

where $\boldsymbol{x}(l)$ is a coordinate vector at the point l. It follows from Eqs. (1) and (4) that near the transition point each quasi-straight piece interacts with a large number of neighbors [$k_{neigh} \sim \rho_c v/a^2 l_p \sim (l_p/a)^{1+\omega/1+2\omega} \gg 1$]. Therefore, the term $U(\boldsymbol{x}, \boldsymbol{s}, \varphi)$ can be obtained by using a self-consisting-field approach [14]. In this region the repulsive and attractive contributions to binary collisions between the molecule's pieces compensate each other and high order collisions become significant [6]. Such compensation, however, takes place only for angular independent contributions, so we should keep higher order terms only for angular independent contributions, while for angular-dependent interactions we could take into account only collisions of the lowest order. Thus, the interaction energy can be approximated as:

$$U \simeq T\varrho(\boldsymbol{x})\left(\oint d\boldsymbol{s'}\, d\varphi'\, \gamma(\boldsymbol{s}-\boldsymbol{s'};\varphi-\varphi')g(\boldsymbol{x},\boldsymbol{s'},\varphi') + \Phi(\varrho(\boldsymbol{x}))\right), \tag{53}$$

where function $g(\boldsymbol{x}, \boldsymbol{s'}, \varphi')$ describes local fraction of quasi-straight segments with twist φ', which are oriented along the direction $\boldsymbol{s'}$. $\varrho(\boldsymbol{x})$ is the local density of the CLM segments near point $\boldsymbol{x}$. $\gamma(\boldsymbol{s}-\boldsymbol{s'};\varphi-\varphi')$ describes the angular-dependent part of energy of interactions, while angle-independent contributions are included in the term $\Phi(\varrho)$. It is assumed that the first term (53) is vanished for $g(\boldsymbol{x}, \boldsymbol{s}, \varphi) = const$. Using the same arguments as in [6, 16], we can consider $\Phi(\varrho)$ as an analytical function and expand it over ϱ:

$$\Phi \simeq \tau + \kappa\varrho. \tag{54}$$

Note, that for the main approximation, higher order terms in (54) should be omitted, because they lead to higher order contributions to the free energy $\sim o\left((a/l_p)^{4\omega/(1+2\omega)}\right)$. $\tau > 0$ corresponds to a good solvent and $\tau < 0$ to a poor solvent and it depends on the chemical composition of the solvent.

It should be noted that because $g(\boldsymbol{x})$ and $\varrho(\boldsymbol{x})$ are slowly changed within the interaction scales, we can use local approximation for the functions γ and Φ. Corresponding contribution to the free energy per unit volume can be found from [26]:

$$\mathcal{F} = -\frac{T\rho}{a^2 L}\ln\int d^3\boldsymbol{x}\oint d\boldsymbol{s}\, d\varphi\, \mathcal{G}(\boldsymbol{s},\varphi,\boldsymbol{x}|\boldsymbol{s},\varphi+2\pi m,\boldsymbol{x};L), \tag{55}$$

where $\mathcal{G}(\boldsymbol{s}_0,\varphi_0,\boldsymbol{x}_0|\boldsymbol{s}_1,\varphi_1,\boldsymbol{x}_1;L)$ is a Green function of Hamiltonian $\mathcal{H}_{PT}$ and $\oint$ designates integration over φ and directions of $\boldsymbol{s}$ and ρ is the average volume fraction of the molecule

(m is an integer number). It can be shown in a standard way [6] (see Appendix 2) that for the first approximation on (a/l_p) and $K_0 l_p$, $\mathcal{G}$ is:

$$\frac{\partial \mathcal{G}}{\partial L} - \widehat{H}\mathcal{G} = \delta(L)\delta(\boldsymbol{s}_1 - \boldsymbol{s}_0)\delta(\boldsymbol{x}_1 - \boldsymbol{x}_0)\delta(\varphi_1 - \varphi_2), \tag{56}$$

with

$$\begin{aligned} \widehat{H} = &-(\boldsymbol{s}\cdot\nabla) - K_0\left(\boldsymbol{A}\cdot\frac{\partial}{\partial \boldsymbol{s}}\right) - \Omega_0\frac{\partial}{\partial\varphi} + \frac{1}{2l_p}\frac{\partial^2}{\partial \boldsymbol{s}^2} \\ &+\frac{1}{2l_t}\frac{\partial^2}{\partial\varphi^2} - \frac{K_0}{2}\frac{\partial \boldsymbol{A}}{\partial \boldsymbol{s}} - \frac{U}{aT}; \\ \boldsymbol{A} = [\boldsymbol{s}\times\boldsymbol{b}] &= \frac{(\boldsymbol{e} - \boldsymbol{s}(\boldsymbol{e}\cdot\boldsymbol{s}))\cos\varphi + [\boldsymbol{e}\times\boldsymbol{s}]\sin\varphi}{\sqrt{1-(\boldsymbol{e}\cdot\boldsymbol{s})^2}}, \end{aligned} \tag{57}$$

where $\partial/\partial\boldsymbol{s}$ and $\partial^2/\partial\boldsymbol{s}^2$ - are gradient and Laplacian over the angular variable $\boldsymbol{s}$, while ∇ is gradient over the space variable $\boldsymbol{x}$, ($\boldsymbol{e}$ is a constant unit vector, which reflects initial orientation of the super-helix. The free energy, of cause, is invariant under arbitrary rotation of $\boldsymbol{e}$).

If $K_0(l), \Omega_0(l)$ are changed slowly on scale l_p, where $\mathcal{G}$ significantly changes (this is typical for bacterial DNA [25]), we can use adiabatic approximation for Green function [26] and write:

$$\mathcal{G} \simeq \sum_i w_i^+(\boldsymbol{s}_1, \varphi_1, \boldsymbol{x}_1) w_i^-(\boldsymbol{s}_0, \varphi_0, \boldsymbol{x}_0) \exp - \int_0^L E_i(K_0(l), \Omega_0(l))dl, \tag{58}$$

where l is considered as an imaginary time and $\{E_i\}$ is the energy spectrum of the equation

$$\widehat{H} w_i \simeq -E_i w_i. \tag{59}$$

$w_i^-(\boldsymbol{s}, \varphi, \boldsymbol{x}) = w_i^+(-\boldsymbol{s}, -\varphi, \boldsymbol{x})$ and they are normalized as $\int w_i^+ w_i^- \, d^3\boldsymbol{x}\, d\boldsymbol{s}\, d\varphi = 1$.

The main contribution to the sum in Eq. (58) is given by the lowest part of the energy spectrum. The structure of this part depends on the ratio of l_p^{-1}, l_t^{-1} to the depth of the "potential well": $\sim (U_{max} - U_{min})/T$. If this ratio is small, the lowest part of the spectrum will be discrete, otherwise it will be continuous. In the high density phase this ratio can be estimated as $T l_p^{-1}/(U_{max} - U_{min}) \sim a/\rho l_p \sim \rho_*/\rho_c$, so, for $\rho_c \gg \rho_*$ the lowest part of the spectrum is discrete. (In the low density phase $\nabla w = 0$ and $U \simeq const.$, and the spectrum is obviously discrete, because $\boldsymbol{s}$ and φ are changed in the finite regions.) Since a gap between the ground and the first exited state is about $E_1 - E_0 \sim l_p^{-1}$, so $[\exp -L(E_1 - E_0)] \sim \exp -L/l_p \ll 1$, we can keep in (58) only the term with the lowest E_0 [15].

Then, free energy is expressed as:

$$\mathcal{F} \simeq \frac{T\rho}{a^2 L}\int_0^L E_0(K_0(l),\Omega_0(l))dl + o(a/L).$$

Rewriting w in the pseudo-polar form:,

$$w(\boldsymbol{s},\boldsymbol{x},\varphi) = u(\boldsymbol{s},\boldsymbol{x},\varphi)\exp[K_0 l_p f(\boldsymbol{s},\boldsymbol{x},\varphi)], \tag{60}$$

where

$$\begin{aligned} u(\boldsymbol{s},\varphi,\boldsymbol{x}) &= \sqrt{w(\boldsymbol{s},\varphi,\boldsymbol{x})w(-\boldsymbol{s},-\varphi,\boldsymbol{x})} \\ K_0 l_p f(\boldsymbol{s},\boldsymbol{x},\varphi) &= \ln\left(\sqrt{w(\boldsymbol{s},\varphi,\boldsymbol{x})/w(-\boldsymbol{s},-\varphi,\boldsymbol{x})}\right), \end{aligned} \tag{61}$$

one obtains (see Appendix 3):

$$\begin{aligned} \mathcal{F} = \frac{T}{a^3}\int d^3\boldsymbol{x}\oint d\boldsymbol{s}\,d\varphi\left\{\frac{a}{2l_p}\left(\frac{\partial u}{\partial \boldsymbol{s}}\right)^2 + \frac{a}{2l_t}\left(\frac{\partial u}{\partial \varphi}\right)^2 + \right. \\ \left. + \left[\frac{U(\boldsymbol{s},\boldsymbol{x},\varphi)}{T} + h\left(\left(\frac{\partial f}{\partial \boldsymbol{s}}\right)^2 + \frac{l_p}{l_t}\left(\frac{\partial f}{\partial \varphi}\right)^2\right)\right]u^2\right\}, \end{aligned} \tag{62}$$

where $h = a l_p \overline{K^2} = a l_p L^{-1}\int_0^L K_0^2 dl$. For DNA molecule h can be estimated as $h \simeq (l_p/2a)\sigma^2\cos^4\beta$ [25], where σ is super-helical density and β is an opening angle of the super-helix.

Expression (62) should be minimized over $u(\boldsymbol{s},\boldsymbol{x},\varphi)$ under restriction (see Appendix 3):

$$\begin{aligned} \left(\frac{\partial}{\partial \boldsymbol{s}}\cdot\left(u^2\frac{\partial f}{\partial \boldsymbol{s}}\right)\right) + \frac{l_p}{l_t}\frac{\partial}{\partial\varphi}\left(u^2\frac{\partial f}{\partial\varphi}\right) = \\ = \left(\frac{\partial}{\partial \boldsymbol{s}}\cdot(u^2\boldsymbol{A})\right) + \frac{\Omega_0}{K_0}\frac{\partial u^2}{\partial\varphi} + \frac{1}{K_0}\left(\nabla\cdot\boldsymbol{s}u^2\right), \\ \int d^3\boldsymbol{x}\oint d\boldsymbol{s}\,d\varphi\,u^2(\boldsymbol{s},\boldsymbol{x},\varphi) = 1 \end{aligned} \tag{63}$$

In order to find the minimum of (62) we will use the Onzager approach [5], where it is assumed that $u = \exp\lambda\psi(\boldsymbol{s},\boldsymbol{x})$ and the function $\psi(\boldsymbol{s},\boldsymbol{x})$ has a maximum in the direction of the local average orientation of quasi-straight segments. The parameter λ is found by minimizing $\mathcal{F}$ and it is assumed that $\lambda > 0$ in the ordered phase and $\lambda = 0$ in the disordered one.

To define factor $\gamma(\boldsymbol{s}-\boldsymbol{s'};\varphi-\varphi')$, note that for $\lambda \gg 1$ (which is correct near the phase transition in our case), the function $u(\boldsymbol{s},\boldsymbol{x})$ has a narrow maximum in the direction of the local average orientation of quasi-straight segments. Because in the used approximation $g = u^2$, the small-angle collisions give the main contribution to the angular-dependent term in (53). This means that the behavior of γ near $|\theta| \ll 1$, where θ is the angle between $\boldsymbol{s}$ and $\boldsymbol{s'}$, is relevant and we will approximate γ as

$$\gamma \simeq \varsigma + \eta|\theta|^{\omega},$$

The constant $\varsigma < 0$ ensures that the average of $\gamma(\boldsymbol{s}-\boldsymbol{s'};\varphi-\varphi')$ is vanished (we will assume later that ς is included in τ). Generally speaking, η is an analytical function of $(\varphi-\varphi')$, but for $\Omega_0 l_t \ll K_0 l_p$ dependence γ on φ can be neglected. For the excluded volume contribution and for the forces that were considered in [21] $\omega = 1$ should be chosen.

The final result depends weakly on the specific form of the prob function u (see Appendix 5) and can be obtained explicitly for $\lambda \gg 1$. Somewhat exhausting but straightforward calculations show that $\lambda \sim [\eta\Gamma(2+\omega)\rho l_p/a]^{1/1+\omega}$, so $\lambda \gg 1$ for $\rho \gg a/l_p$. (Here Γ is Gamma function). Finally one obtains

$$\mathcal{F} \simeq Ta^{-3}\left[\left(\tilde{a}/l_p\right)^{\alpha}\rho^{2-\alpha} + \tau\rho^2 + \kappa\rho^3 + h\rho\right], \tag{64}$$

with $\alpha = \omega/1+\omega$ and $\tilde{a} \sim [\eta\Gamma(2+\omega)]^{1/\omega}a$.

It is easy to show (see Appendix 4) that near point:

$$\tau_c \simeq -2\kappa\rho_c\left\{1 + (1-\alpha)\left(\frac{\alpha\sigma}{\kappa\sigma_c}\Lambda\right)^{-1/1+\alpha}\right\}, \tag{65}$$

where $\sigma_c \simeq [(\eta\Gamma(2+\omega))^{-1/2\omega}\alpha^{(3+\alpha)/2(1+\alpha)}\cos^{-2}\beta]\kappa^{(\alpha-1)/2(1+\alpha)}(\tilde{a}/l_p)^{(1+3\alpha)/2(1+\alpha)}$, the system undergoes the first order liquid-crystal phase transition with critical volume fraction of the molecule:

$$\rho_c \simeq c_o\left(\frac{\tilde{a}}{l_p}\right)^{\alpha/1+\alpha}\frac{\sigma}{\sigma_c}\Lambda\left(\frac{\sigma}{\sigma_c}\right), \tag{66}$$

where $c_o \simeq (\alpha/\kappa)^{1/1+\alpha}$ and function Λ satisfies to

$$(\sigma_c/\sigma)^{1+\alpha}\Lambda^{1-\alpha} - \Lambda^2 + 1 = 0. \tag{67}$$

It has an asymptotic:

$$\Lambda\left(\frac{\sigma}{\sigma_c}\right) \simeq \begin{cases} \sigma_c/\sigma \text{ for } \sigma \ll \sigma_c \\ 1 \quad \text{for } \sigma \gtrsim \sigma_c \end{cases}$$

The jump of entropy near the transition point is:

$$\Delta S_c = q/T \sim (\tilde{a}/l_p)^{2\alpha-1/1+\alpha} \rho_c^{2-\alpha}, \tag{68}$$

where q is latent heat and it is relatively small, while a jump of the liquid-crystal order parameter

$$\mathcal{Q}_c \simeq 1 - \frac{3}{\lambda(\rho_c)} \sim 1$$

is large.

It is clearly seen that there is a well defined critical value of the super-helical density - σ_c, that alters the transition properties. For $\sigma \ll \sigma_c$ the transition's parameters are independent of the super-helical density:

$$\tau_c \sim -\kappa \left(\frac{\tilde{a}}{l_p}\right)^{\alpha/1+\alpha},$$
$$\rho_c \sim \left(\frac{\tilde{a}}{l_p}\right)^{\alpha/1+\alpha},$$

and the phase transitions in the closed and the open macromolecule are the same. However, in the opposite case $\sigma_c \lesssim \sigma$ the situation is cardinally changed:

$$\tau_c \sim -\kappa \left(\frac{\tilde{a}}{l_p}\right)^{\alpha/1+\alpha} \frac{\sigma}{\sigma_c}\left[1 + o\left((\sigma_c/\sigma)^{1/1+\alpha}\right)\right],$$
$$\rho_c \sim \left(\frac{\tilde{a}}{l_p}\right)^{\alpha/1+\alpha} \frac{\sigma}{\sigma_c},$$

so, super-helical density becomes one of the major factors that influence the crystallization process. This case corresponds to bacterial DNA, where the crossover value $\sigma_c \sim 5 \cdot 10^{-3}$ is very small, while typical values of the super-helical density are $\sigma \sim 5 \cdot 10^{-2} \gg \sigma_c$. It can be seen that super-helicity doesn't prevent phase transition to the crystalline state but decreases the transition point and increases sharpness of the phase transition. Qualitative behavior of $\rho(\tau), \rho_c(\sigma), \tau_c(\sigma)$ and $Q_c(\sigma)$ is shown in Fig. 6. It should be noted that free energy (64) contains only bulk contribution, because the surface contribution is proportional to $(\rho a/L)^{1/3}$ and should be neglected in the used approximation.

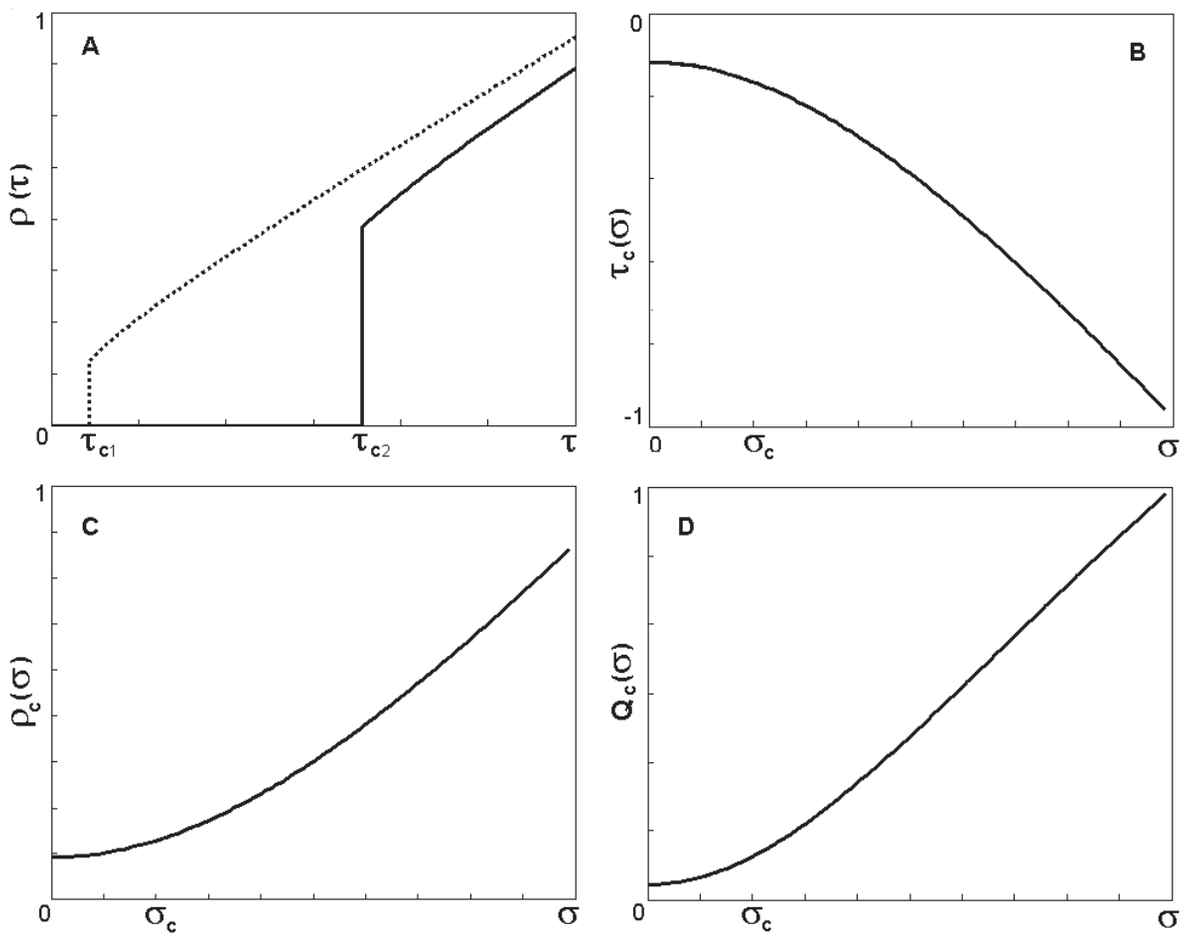


Figure 6. Behavior of the transition's parameters. **A** - behavior of $\rho(\tau)$ for different σ. Dashed line $\sigma = 0$, solid line $\sigma \gg \sigma_c$. **B** behavior of $\tau_c(\sigma)$, **C** - behavior of $\rho_c(\sigma)$, **D** - behavior of $Q_c(\sigma)$. Reproduced with permission from Ref.[15].

It should be emphasized that condition $a/l_p \ll 1$ is essential for liquid-crystal ordering. Although our approach is not quantitatively validated for $a/l_p \sim 1$, one can hope that it qualitatively correctly predicts the behavior of the system characteristics in this limit. Since for $a \sim l_p$ it should take $\lambda = 0$, the liquid crystal ordering should not take place in this case.

6. Discussion

The MFA is the most crucial approximation in our theory but it is a reasonable one. At low temperatures each quasi-straight piece of a fiber or collagen molecule interacts with a large number of neighbors and, therefore, fluctuations of the concentration are irrelevant. On the other hand, the phase transitions are of the first order and fluctuations of the order parameter are therefore small. Note, that main assumptions, which have been used in the Sec.4, are general enough to apply the theory to a class of compressed materials made from various fibers. It could be used, for example, for implant materials made from actin myofibrils or for artificial wood made from natural cellulose fibrils.

It has been shown in [12], [2], that a novel material can be developed by exerting high pressure and temperature on natural leather material. The production is done in an oxygen poor environment in order to prevent burning of the leather. The resulting material, which was called *pleather*, is thermoplastic.

For low pressure, heating leads to destruction of the leather, but for high pressure it leads to the appearance of an amorphous material. This transformation corresponds to the transition described here. For this transition the jump of Young's modulus is strongly correlated with the jump in the compressibility. The theory predicts the stabilization of the spiral form of the collagen molecules at high pressure and the sensitivity of the transition to an uniaxial stress [10]. The spiral form stabilization has been found already in an aqueous solution of collagen [11], while the sensitivity to an uniaxial stress should be tested by experiment. Other predictions of the theory like positive shift of the transition temperature with pressure and small latent heat of the transitions are in good agreement with the experimental observations [12], [2] as well.

It should be noted, that in the real material the phase transition under heating is not reversible and after cooling the system does not return to the initial low-temperature phase. This effect is connected with the cross-links between collagen molecules in the coil form. These cross-links are not important for the behavior under heating, because until the phase transition the spirality of collagen is large. However, if we cool the material after phase transition the cross-links prevents spiralization and, therefor, stabilize the disordered phase.

Considering the bacterial DNA crystallization, one can say [28] that the cellular conditions that determine super-helical parameters regulate the packaging of DNA as well and, therefore, regulate bacterial endurance and virulence. The theory predicts crucial role of super-helicity in DNA condensation, which has been found experimentally [19, 24, 28]. It was found also that the condensation conditions of closed (with $\sigma \simeq 3 \cdot 10^{-2}$) and of open DNA are different [19]. For $\omega = 1$, which looks reasonable in the considered situation, $\rho_c \sim 0.4$ and $Q_c \sim 0.75$ are in qualitative agreement with the experimental observation.

Apparently, the situation $a/l_p \sim 1$ is realized in eucaryote cells, where the initial phase of DNA packing is presented by fiber that comprises a string of repeating units: the nucleosomes, where DNA molecules wind around histone cores. The nucleosomes are connected by pieces of free DNA, so the flexibility of the fiber is close to the flexibility of the DNA chain, while the fiber's effective diameter is approximately of nucleosome size: $a_{nucl} \sim l_p$, so there is no liquid crystal crystallization. In fact, in this situation, the "beads on string" model [16] seems more appropriate. It is shown [16] that in this case an ordinary collapse of the chain to a friable, non-crystalline state must occur. This supports the hypothesis [29] that nucleosomes were formed to counteract spontaneous transition of the eucaryotic DNA into crystalline state.

Acknowledgment

I would like to thank Prof. A.Wyler (JCT) for fruitful collaboration. I thank also Prof. A.Minsky (Weizmann Institute of Science), who set forth the biological importance of the bio-crystallization and explained the experimental situation to me. Without his help and comments theory of DNA crystallization could not have been done.

Appendix 1

We have for $\lambda \gg 1$:

$$F \simeq F_0 + \frac{\chi T c^2}{2D^3} \int\limits_0^1 dx \left(\frac{TD}{\chi \gamma c} \left(1 - x^2\right) A\lambda^2 \left(\phi'(x)\right)^2 \exp\left(\lambda\phi(x)\right) + \right.$$
$$\left. + 2^\omega \kappa A^2 \exp\left(\lambda\phi(x)\right) \int\limits_0^1 dy \exp\left(\lambda\phi(y)\right) |x-y|^\omega P_\omega \left(\left| \frac{2-x-y}{x-y} \right| \right) \right).$$

where

$$\kappa = \lim_{\vec{n} \to \boldsymbol{k}} \frac{u(\boldsymbol{n}, \boldsymbol{k})}{|\boldsymbol{n} \times \boldsymbol{k}|^{2\omega}},$$
$$\omega = \lim_{\boldsymbol{n} \to \boldsymbol{k}} \frac{1}{2} \frac{\partial \ln u(\boldsymbol{n}, \boldsymbol{k})}{\partial \ln |\boldsymbol{n} \times \boldsymbol{k}|}.$$

and P_ω is a Legendre function. Since the main contribution to these integrals gives $x \sim y \sim 1$ we can put: $\phi(y) \simeq \phi(1) - \phi'(1)(1-y) + o\left((1-y)^2\right) \simeq \phi(1) - u + o\left(u^2\right)$ and obtain for the coefficient $\zeta(\omega)$

$$\zeta = 2^\omega \kappa \int_0^\infty du dz e^{-u-z} |u-z|^\omega P_\omega \left(\left| \frac{u+z}{u-z} \right| \right) + o\left(e^{-\lambda}\right) \simeq$$
$$\simeq 2^{\omega+2} \kappa \int\limits_0^\infty du' dz' \ (uz) e^{-u'^2 - z'^2} \left| u'^2 - z'^2 \right|^\omega P_\omega \left(\left| \frac{u'^2 + z'^2}{u'^2 - z'^2} \right| \right) =$$
$$= 2^{\omega+2} \kappa \int\limits_0^{2\pi} d\varphi \ \sin\varphi \cos\varphi \left| \sin^2\varphi - \cos^2\varphi \right|^\omega P_\omega \left(\left| \frac{1}{\sin^2\varphi - \cos^2\varphi} \right| \right) \times$$
$$\times \int\limits_0^\infty dr \, r^{2(1+\omega)+1} \exp\left(-r^2\right)$$
$$= 2^{\omega-1} \kappa \int\limits_0^\infty dx \, x^{1+\omega} e^{-x} \int\limits_0^\pi d\phi \ \sin\phi |\cos\phi|^\omega P_\omega \left(\left| \frac{1}{\cos\phi} \right| \right) =$$
$$\simeq 2^\omega \kappa \Gamma(2+\omega) \int\limits_1^\infty dz \, z^{-2-\omega} P_\omega(z).$$

where $\Gamma(x)$ is Gamma function. So

$$\zeta(\omega) = 2^{2\omega} \Gamma(1+\omega) \kappa.$$

If the term $|\boldsymbol{n} \times \boldsymbol{k}|^{2\omega}$ gives the main contribution to $u(\boldsymbol{n}, \boldsymbol{k})$, we obtain

$$\kappa \approx \frac{2\Gamma\left(\frac{3}{2}+\omega\right)}{\sqrt{\pi}\Gamma(1+\omega)},$$

and for $\omega \leq 1$

$$\zeta(\omega) \approx 2^{2\omega}(1-0.02\omega).$$

Appendix 2

Green function $\mathcal{G}(\boldsymbol{s}_0, \varphi_0, \boldsymbol{x}_0 | \boldsymbol{s}_1, \varphi_1, \boldsymbol{x}_1; L)$ is defined as:

$$\mathcal{G}(\boldsymbol{s}_0, \varphi_0, \boldsymbol{x}_0 | \boldsymbol{s}_1, \varphi_1, \boldsymbol{x}_1; L) = \underbrace{\int\int}\mathfrak{D}\boldsymbol{x}(l)\boldsymbol{s}(l)\varphi(l)\ \exp -\frac{H_{PT}(L)}{T},$$

$$\text{with: } \boldsymbol{x}(0)=\boldsymbol{x}_0;\ \boldsymbol{s}(0)=\boldsymbol{s}_0;\ \varphi(0)=\varphi_0; \qquad \boldsymbol{x}(L)=\boldsymbol{x}_1;\ \boldsymbol{s}(L)=\boldsymbol{s}_1;\ \varphi(L)=\varphi_1,$$

where $\underbrace{\int\int}\mathfrak{D}\boldsymbol{x}(l)\boldsymbol{s}(l)\varphi(l)$ is a path integral over all possible shapes of a molecule chain. This Green function satisfies the equation [6] (see Fig. 7):

$$\mathcal{G}(\boldsymbol{s}_0, \varphi_0, \boldsymbol{x}_0 | \boldsymbol{s}, \varphi, \boldsymbol{x}; L) = \int\oint d^3\boldsymbol{x}'\, d\boldsymbol{s}'\, d\varphi'\, \mathcal{G}(\boldsymbol{s}_0, \varphi_0, \boldsymbol{x}_0 | \boldsymbol{s}', \varphi', \boldsymbol{x}'; L-dL)$$
$$\mathcal{G}(\boldsymbol{s}', \varphi', \boldsymbol{x}' | \boldsymbol{s}, \varphi, \boldsymbol{x}; dL). \tag{69}$$

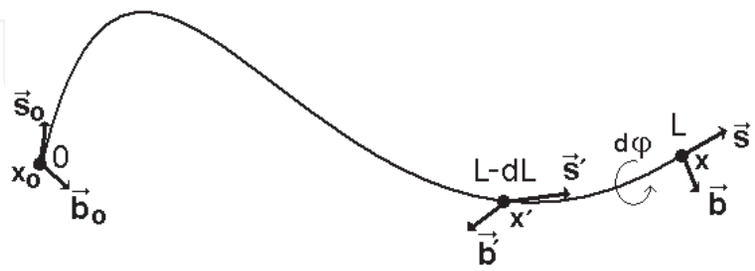


Figure 7. To equation (69). L is a macromolecule's contour length, persistent lengths, $\boldsymbol{s}_0, \boldsymbol{s}', \boldsymbol{s}$ are unit tangent vectors, $\boldsymbol{b}_0, \boldsymbol{b}', \boldsymbol{b}$ are unit bi-normal vectors, φ is the twist angle and $\boldsymbol{x}_0, \boldsymbol{x}$ are coordinate vectors at initial and end points of the molecule. Reproduced with permission from Ref.[15].

If dL is small the function $\mathcal{G}(\boldsymbol{s}', \varphi', \boldsymbol{x}' | \boldsymbol{s}, \varphi, \boldsymbol{x}; dL)$ can be presented as:

$$\mathcal{G}(\boldsymbol{s'},\varphi',\boldsymbol{x'}|\boldsymbol{s},\varphi,\boldsymbol{x};dL) \simeq \frac{1}{Z}\exp-\left\{\frac{l_p}{2}\left[\frac{\boldsymbol{s}-\boldsymbol{s'}}{dL}-\boldsymbol{K}\left(\frac{\boldsymbol{s}+\boldsymbol{s'}}{2},\frac{\varphi+\varphi'}{2},L-\frac{dL}{2}\right)\right]^2\right.$$
$$+\frac{l_t}{2}\left[\frac{\varphi-\varphi'}{dL}-\Omega_0\left(L-\frac{dL}{2}\right)\right]^2+$$
$$\left.+\frac{1}{aT}U\left(\frac{\boldsymbol{s}+\boldsymbol{s'}}{2},\frac{\varphi+\varphi'}{2},\frac{\boldsymbol{x}+\boldsymbol{x'}}{2}\right)\right\}dL, \tag{70}$$

where Z is a proper normalization multiplier. Observing that $\boldsymbol{x'}=\boldsymbol{x}-\boldsymbol{s}dL$ and symbolling:

$$\sqrt{dL}\boldsymbol{p}=\boldsymbol{s}-\boldsymbol{s'}-\boldsymbol{K}dL,$$
$$\sqrt{dL}t=\varphi-\varphi'-\Omega dL,$$

and keeping in (70) the lowest on dL terms one obtains:

$$\mathcal{G}(\boldsymbol{s'},\varphi',\boldsymbol{x'}|\boldsymbol{s},\varphi,\boldsymbol{x};dL) \simeq \frac{1}{Z}\left[1-\frac{l_p}{2}\left(\boldsymbol{p}\cdot\left(\boldsymbol{p}\cdot\frac{\partial}{\partial\boldsymbol{s}}\right)\boldsymbol{K}\right)dL-\frac{l_p}{2}t\left(\boldsymbol{p}\cdot\frac{\partial\boldsymbol{K}}{\partial\varphi}\right)dL-\right.$$
$$\left.-\frac{l_t}{2}\left(t^2\frac{\partial\Omega_0}{\partial L}\right)dL+\frac{U(\boldsymbol{s},\varphi,\boldsymbol{x})}{aT}dL\right]\exp-\left(\frac{l_p\boldsymbol{p}^2}{2}+\frac{l_pt^2}{2}\right). \tag{71}$$

Correspondingly, for $\mathcal{G}(\boldsymbol{s}_0,\varphi_0,\boldsymbol{x}_0|\boldsymbol{s'},\varphi',\boldsymbol{x'};L-dL)=\mathcal{G}(\boldsymbol{s}_0,\varphi_0,\boldsymbol{x}_0|\boldsymbol{s}-\sqrt{dL}\boldsymbol{p}-\boldsymbol{K}dL,\varphi-\sqrt{dL}t-\Omega_0dL,\boldsymbol{x}-\boldsymbol{s}dL;L-dL)$ one has

$$\mathcal{G}(\boldsymbol{s}_0,\varphi_0,\boldsymbol{x}_0|\boldsymbol{s'},\varphi',\boldsymbol{x'};L-dL) \simeq \mathcal{G}(\boldsymbol{s}_0,\varphi_0,\boldsymbol{x}_0|\boldsymbol{s},\varphi,\boldsymbol{x};L)+$$
$$+\left[\frac{\boldsymbol{p}^2}{2}\frac{\partial^2\mathcal{G}}{\partial\boldsymbol{s}^2}=\frac{t^2}{2}\frac{\partial^2\mathcal{G}}{\partial\varphi^2}-\frac{\partial\mathcal{G}}{\partial L}-\right.$$
$$-\left([\boldsymbol{K}+dL^{-1/2}\boldsymbol{p}]\cdot\frac{\partial\mathcal{G}}{\partial\boldsymbol{s}}\right)-[\Omega_0+dL^{-1/2}t]\frac{\partial\mathcal{G}}{\partial\varphi}-(\boldsymbol{s}\cdot\nabla\mathcal{G})-$$
$$\left.-\frac{1}{2}t\left(\boldsymbol{p}\cdot\frac{\partial^2\mathcal{G}}{\partial\boldsymbol{s}\partial\varphi}\right)\right]dL. \tag{72}$$

Substituting (71),(72) to (69) and integrating over $(\boldsymbol{p},t)$ one obtains (56),(57).

Appendix 3

Using (60) in (59) and taking into account that $u(-\boldsymbol{s},-\varphi,\boldsymbol{x})=u(\boldsymbol{s},\varphi,\boldsymbol{x})$; $f(-\boldsymbol{s},-\varphi,\boldsymbol{x})=-f(\boldsymbol{s},\varphi,\boldsymbol{x})$, one obtains:

$$
\begin{aligned}
-Eu(\pm\boldsymbol{s},\pm\varphi,\boldsymbol{x}) = {} & \frac{1}{l_p}\left(\frac{\partial^2 u}{\partial \boldsymbol{s}^2}\right)+\frac{1}{l_t}\left(\frac{\partial^2 u}{\partial \varphi^2}\right)+K_0 l_p\left[\Omega_0\frac{\partial f}{\partial\varphi}+\left(\boldsymbol{K}\cdot\frac{\partial f}{\partial \boldsymbol{s}}\right)+(\boldsymbol{s}\cdot\nabla f)\right]u \\
& + \left[K_0^2 l_p^2\left(\frac{1}{l_p}\left(\frac{\partial f}{\partial \boldsymbol{s}}\right)^2+\frac{1}{l_t}\left(\frac{\partial f}{\partial\varphi}\right)^2\right)+\frac{1}{2}\frac{\partial\Omega_0}{\partial l}-\frac{U}{aT}\right]u+ \\
& \pm\left\{-\Omega_0\frac{\partial u}{\partial\varphi}-\frac{1}{2}\frac{\partial \boldsymbol{K}}{\partial \boldsymbol{s}}u-(\boldsymbol{s}\cdot\nabla u)-\left(\boldsymbol{K}\cdot\frac{\partial u}{\partial \boldsymbol{s}}\right)+\right. \\
& + K_0 l_p\left[\frac{1}{l_p}\left(\frac{\partial u}{\partial \boldsymbol{s}}\cdot\frac{\partial f}{\partial \boldsymbol{s}}\right)+\frac{1}{l_t}\left(\frac{\partial u}{\partial\varphi}\frac{\partial f}{\partial\varphi}\right)+\right. \\
& \left.\left.+\ \frac{1}{2l_p}\left(\frac{\partial^2 f}{\partial \boldsymbol{s}^2}\right)u+\frac{1}{2l_t}\left(\frac{\partial^2 f}{\partial\varphi^2}\right)u\right]\right\}.
\end{aligned}
\tag{73}
$$

Subtracting the expressions with different signs one obtains (63). Summing the expressions with different signs, multiplying both sides by $u(\boldsymbol{s},\varphi,\boldsymbol{x})$ and integrating over $\boldsymbol{s},\varphi,\boldsymbol{x}$ and dl/L one obtains (62).

Actually, restriction (63) ensures that w_0^+ and w_0^- have the same eigenvalue E_0. Indeed, it follows from (73) and (63) that $w_0^+\hat{H}w_0^- = w_0^-\hat{H}w_0^+$. Let us assume that:

$$
\begin{aligned}
-E_0^+ w_0^+ &= \hat{H}w_0^+, \\
-E_0^- w_0^- &= \hat{H}w_0^-.
\end{aligned}
$$

Multiplying the first equation by w_0^- and the second by w_0^+ one obtains:

$$
(E_0^+ - E_0^-)w_0^- w_0^+ = w_0^+\hat{H}w_0^- - w_0^-\hat{H}w_0^+ = 0.
$$

So, $E_0^+ = E_0^- = E_0$.

Appendix 4

Since $\mathcal{F}(\rho)$ in Eq (64) is not singular for any positive ρ, phase transition to the crystalline state can be only of a first order. The transition point τ_c and jump of volume fraction of the molecule ρ_c should be found from the conditions:

$$
\begin{aligned}
\mathcal{F}(\rho_c) &= \mathcal{F}(0), \\
\frac{\partial\mathcal{F}}{\partial\rho_c} &= 0,
\end{aligned}
$$

or

$$\left(\tilde{a}/l_p\right)^{\alpha}\rho_c^{1-\alpha}+\tau_c\rho_c+\kappa\rho_c^2+h=0,$$
$$(2-\alpha)\left(\tilde{a}/l_p\right)^{\alpha}\rho_c^{1-\alpha}+2\tau_c\rho_c+3\kappa\rho_c^2+h=0,$$

which after simple algebraic transformations lead to Eqs. (65)-(67).

Appendix 5

Various forms of $\psi(\boldsymbol{s},\boldsymbol{x})$, corresponding to different structures of condensed phases, have been checked. For laminar-like ordering this function can be chosen in the form of:

$$\psi\sim-[\boldsymbol{s}\times\boldsymbol{e}]^2,$$

for toroid-like ordering it is:

$$\psi\sim-(\boldsymbol{s}\cdot\boldsymbol{e})^2-([\boldsymbol{s}\times\boldsymbol{e}]\cdot[\boldsymbol{e}\times\boldsymbol{x}])^2/[\boldsymbol{e}\times\boldsymbol{x}]^2,$$

while for cholesteric ordering it is :

$$\psi\sim-\left([\boldsymbol{s}\times\boldsymbol{k}]\cos(2\pi q(\boldsymbol{e}\cdot\boldsymbol{x}))+[\boldsymbol{s}\times\boldsymbol{p}]\sin(2\pi q(\boldsymbol{e}\cdot\boldsymbol{x}))\right)^2,$$

where $1/q\gg1$ is a cholesteric repeat, $|\boldsymbol{k}|=|\boldsymbol{p}|=1$, $\boldsymbol{e}=[\boldsymbol{k}\times\boldsymbol{p}]$ and $(\boldsymbol{k}\cdot\boldsymbol{p})=0$. With accuracy to slight variance in the numerical coefficients, all forms of $\psi(\boldsymbol{s},\boldsymbol{x})$ lead to the same expression for the free energy. This means that the Onzager approach is unreliable concerning information about the specific structure of the crystalline state. On the other hand, this approach gives a reasonable approximation the for thermodynamic properties of the phase transition.

Author details

Uziel Sandler

Jerusalem College of Technology, Jerusalem, Israel

References

[1] B. de Castro, M.Ferreira , R.T.Markus and A.Wyler, Influence of Prossesing Temperature and Pressure on Stability of the Structure of Hot Pressed Ground Leather, J.Macromol. Sci. ,1997, A34(1), 109-112.

[2] A.Wyler, R.T.Markus and B.de Castro B. , A Model for the Internal Structure of Hot Pressed Leather, J. Soc. Leather Technol. and Chem., 75, (1991), 52-55.

[3] K. Gekko and M. Fukamizu, Int.J.Biol.Macromol, 1991, 13, 295-300.

[4] P. Fratzl *et. al.*, Fibrillar Structure and Mechanical Properties of Collagen, J. of Structeral Biol., 1997, 122, 119Ű122.

[5] P.G.de Gennes ,The Physics of Liquid Crystals. Oxford: Clarendon Press; 1974.

[6] P.G.de Gennes, Scaling Concepts in Polymer Physics, Ithaca and London: Cornell Univ.Press; 1979.

[7] A. Khohlov, Concept of Quasimonomers and Its Application to Some Problems of Polymer Statistics. Polymer, 1978, 9, 1387.

[8] P. Kronick, Fundamentals of Leather Manufacturing, ed.E.Heideman, Ch.4, Darmstadt, Germany: Edward Roether KG. Publ.; 1993.

[9] A.A. Vedenov, The Physics of Solutions, Contemporary Problems in Physics, Science, Moscow; 1984; D. Poland, H.A. Scherada, Theory of Helix-Coil Transitions in Biopolymers, New York: Academic Press; 1970.

[10] P.G.de Gennes, (private communication).

[11] K. Gekko and M. Fukamizu, Int.J.Biol.Macromol, , 1991, 13,299.

[12] B. de Castro, M.Ferreira , R.T.Markus and A.Wyler, J.Macromol. Sci., 1997, A34(1), 109.

[13] A.R. Khokhlov, A.N. Semenov, Liquid-Crystalline Ordering in the Solution of. Partially Flexible Macromolecules, Physica A 112, 1982, 605-614; A.R. Khokhlov, A.N. Semenov, On the Theory of Liquid-Crystalline Ordering of Polymer Chains with limited flexibility, J.Stat.Phys., 1985, 38, 161-182; Zheng Yu Chen, Nematic Ordering in Semiflexible Polymer Chains, Macromolecules, 1993, 12, 3419-3423; H. Noguchi, K. Yoshikawa, Folding path in a semiflexible homopolymer chain: A Brownian dynamics simulation, J.Chem.Phys, , 2000, 113, 854-862 (and references there).

[14] U. Sandler, A. Wyler, Phase Transitions under Pressure in Collagenous Material, Phys.Rev.Lett., 1995, 74, 3073-3076; Phase transitions in fiber materials, Phys.Rev.B, 2000, 61, 16-19.

[15] U. Sandler U, Theory of Crystallization of a Closed Macromolecule, Inter. J. of Biological Macromolecules (IJBIOMAC), 2010, 47, 439-444.

[16] I.M. Lifshitz, A.Yu. Grosberg, A.R. Khokhlov, Some problems of the statistical physics of polymer chains with volume interaction, Rev.Mod.Phys, 1978, 50, 684-713.

[17] A. Minsky, E. Shimoni, D. Frenkiel-Krispin, Stress, order and survival, Nature Rev. Mol. Cell Biol,2002, 3, 50-60.

[18] S. Levin-Zaidman, D. Frenkiel-Krispin, E. Shimoni, I. Sabanay, S. G. Wolf and A. Minsky, Ordered intracellular RecAŰDNA assemblies: A potential site of in vivo RecA-mediated activities, PNAS,2000, 97, 6791 - 6796.

[19] C.L. Ma,V.A. Bloomfield, Condensation of supercoiled DNA induced by $MnCl_2$, Biophys.J., 1994,67, 1678-1681.

[20] V.A. Bloomfield, DNA condensation, Curr.Opin.Struct.Biol., 1996, 6, 334-341.

[21] A.A. Kornyshev, S. Leikin, Electrostatic interaction between long, rigid helical macromolecules at all interaxial angles, Phys.Rev.E, 2000, 62, 2576-2596.

[22] F. Livolante, A. Leforestier, Condensed phases of DNA: structures and phase transitions, Prog.Polym.Sci., 1996, 21, 1115-1164.

[23] N.R. Cozzarelli, T.C. Boles, and White, J.H., Primer on the Topology and Geometry of DNA Supercoiling, in: N.R. Cozzarelli, J.C. Wang, (Eds.), DNA Topology and Its Biological Effects, NY: Cold Spring Harbor Laboratory Press, Cold Spring Harbor, 1990, 139-184.

[24] J. Torbet and E. DiCapua, Supercoiled DNA is interwound in liquid crystalline solutions, The EMBO Journal, 1989, 8, 4351-4356.

[25] T.C. Boles, J.H. White and N.R. Cozzarelli, Structure of plectonemically supercoiled DNA, J. Mol. Biol. 1990, 213 931-951.

[26] A.A. Abrikosov, A.P. Gor'kov, M.E. Dzyaloshinskii, Quantum field theoretical methods in statistical physics, 2ed., Pergamon; 1965.

[27] M. Takahashi, K. Yoshikawa, V.V. Vasilevskaya, and A.R. Khokhlov, Collapse of single DNA molecule in poly(ethylene glycol) solutions. J. Chem. Phys. 1995, 102, 6595-6602; S. Kidoaki, K. Yoshikava, Folding and unfolding of a giant duplex-DNA in a mixed solution with polycations, polyanions and crowding neutral polymers, Biophys.Chem., 1999, 76, 133-143.

[28] Z. Reich, E.J. Wachtel, and A. Minsky, Liquid-crystalline mesophases of plasmid DNA in bacteria, Science, 1994, 264, 1460-1463; S.S. Zacharova *et al.*, Liquid Crystal Formation in Supercoiled DNA Solutions, Biophys.J., 2002, 83,1119-1129.

[29] A. Minsky, R. Ghirlando, Z. Reich, Nucleosomes a Solution to a Crowded Intracellular Environment, J.Theor.Biol., 1997, 188, 268-274.